PHYSICAL REVIEW A **109**, 043702 (2024)

One-photon and two-photon blockades in a four-wave-mixing system embedded with an atom

Yuanchuan Li, Zhihai Yao, and Hui Yang*

Department of Physics, Changchun University of Science and Technology, Changchun 130000, China

(Received 17 October 2023; accepted 14 March 2024; published 1 April 2024)

In this paper, the photon blockade effect in a nondegenerate four-wave-mixing system embedded with a two-level atom has been studied. By using an analytical calculation and numerical analysis, we find that both one-photon and two-photon blockade effects could be realized in this system by adjusting the parameters of the system. That is, (i) when the four-wave-mixing interaction and the atom-cavity coupling strength are not equal, the system can realize a one-photon blockade; (ii) when they are consistent with each other, the system can realize a two-photon blockade. In addition, we also discuss the influence of different parameters on the photon blockade effect in detail. The results show that the system constructed in this paper not only could enhance the one-photon blockade effect decisively, but also could implement a two-photon blockade easily with a well-designed energy-level structure, and evidently the blockade effect depends on the parameters of the system. All the results may provide theoretical references for single-photon and multiphoton sources or devices in designing future experiments and practical applications.

DOI: 10.1103/PhysRevA.109.043702

I. INTRODUCTION

With the rapid developments of quantum optics and quantum information science, photon sources [1–4] have been widely used in quantum communication, quantum information technology, quantum computation, and other fields [5–8]. As one of the effective physical methods to obtain stable photon sources, the photon blockade effect [9–18] has been studied intensely. The photon blockade effect is essentially a photon antibunching effect. For a single-photon blockade, the single photon inside the cavity blocks the transmission of further photons so that the photons could be emitted one by one. For a multiphoton blockade, the photons inside the cavity could also block further photons to produce a photon steam. Up to now, a single-photon blockade has been realized in various systems, such as circuit-QED systems [19–21], optomechanical systems [22–24], atom-cavity systems [25–27], and so on, while a multiphoton blockade, which is more challenging, has also been implemented in several systems, such as the Jaynes-Cummings (JC) model [28–30], Kerr-type nonlinear cavities [31–33], an atom-driven cavity-QED system [34], and so on.

The photon blockade effect could also be divided into a conventional photon blockade (CPB) [35–42] and unconventional photon blockade (UPB) [43–46] due to different physical mechanisms of the blockade. The physical mechanism of the formation of CPB is the anharmonic energy ladder which requires strong nonlinearity, while the physical mechanism of the realization of UPB is the destructively quantum interference between different paths with weak nonlinearity. Up to now, both the CPB and UPB have been predicted in many different systems including coupled nonlinear cavities [47–49], quantum-dot-cavity systems [50–52], cavities with second- or third-order nonlinear materials [53,54], and so on.

For realizations of different kinds of photon blockades, appropriate energy-level structures are always the key, so more and more research has aimed to design new schemes with novel energy-level structures to implement different kinds of blockades [55–57]. Recently, we have investigated the CPB in a four-wave-mixing system with Kerr nonlinearity [58]. The results show that a strong single-photon blockade effect could be realized in this system. Inspired by this, in this paper we construct a combined system based on the four-wave interaction to implement the photon blockade effect. The hybrid system is a nondegenerate four-wave-mixing system embedded with a two-level atom which could introduce more nonlinearity. The energy-level structure of this system could be designed by adjusting the interaction strengths. Then different kinds of photon blockade effects could be realized in this system. We investigate the one-photon and two-photon blockade effects in this system analytically and numerically, and obtain the conditions for realizations of different kinds of blockades in this system decisively. In addition, the influence of parameters of the system on the effect of the blockade is discussed in detail.

The rest of this paper is organized as follows. The physical model is introduced in Sec. II. The analytical conditions for the photon blockade are presented in Sec. III. In Sec. IV, the numerical results on the one-photon and the two-photon blockade effects are discussed. Finally, the conclusions are summarized in Sec. V.

II. PHYSICAL MODEL

In this paper, the system we construct here is a nondegenerate four-wave-mixing system embedded with a two-level atom. As shown in Fig. 1, the system consists of two cavities.

*yangh@cust.edu.cn

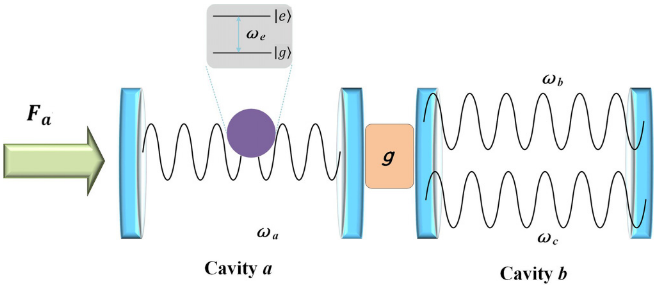

FIG. 1. Schematic illustration of a nondegenerate four-wave-mixing system embedded with a two-level atom. ω_a is the frequency of mode a, and ω_b is the frequency of mode b, while ω_c is the frequency of mode c. ω_e is the atomic transition frequency between the ground state $|g\rangle$ and the excited state $|e\rangle$, and g describes the four-wave-mixing interaction. F_a is the driving strength for the cavity a.

The four-wave-mixing interaction between the two cavities could convert two photons with frequency ω_a in cavity a into one photon with frequency ω_b and the other photon with frequency ω_c in cavity b. In addition, cavity a is embedded with a two-level atom with frequency ω_e and is pumped by an external driving light field with frequency ω_l. Then the Hamiltonian of the system can be described as (setting $\hbar = 1$)

$$\begin{aligned}\hat{H} =\ & \omega_a\hat{a}^\dagger\hat{a} + \omega_b\hat{b}^\dagger\hat{b} + \omega_c\hat{c}^\dagger\hat{c} + g(\hat{a}^{\dagger 2}\hat{b}\hat{c} + \hat{a}^2\hat{b}^\dagger\hat{c}^\dagger) \\ & + \omega_e\hat{\sigma}_+\hat{\sigma}_- + J(\hat{a}^\dagger\hat{\sigma}_- + \hat{\sigma}_+\hat{a}) + F_a(\hat{a}^\dagger e^{-i\omega_l t} + \hat{a}e^{i\omega_l t}),\end{aligned} \tag{1}$$

where $\hat{a}^\dagger$ ($\hat{a}$), $\hat{b}^\dagger$ ($\hat{b}$), and $\hat{c}^\dagger$ ($\hat{c}$) denote the creation (annihilation) operators of modes a, b, and c, respectively, and $\hat{\sigma}_+$ ($\hat{\sigma}_-$) is the raising (lowering) operator of the two-level atom. J denotes the coupling strength between the atom and cavity mode a, while g describes the four-wave-mixing interaction with F_a the driving strength for cavity mode a.

Considering the rotating frame, the effective Hamiltonian can be written as

$$\begin{aligned}\hat{H} =\ & \triangle_a\hat{a}^\dagger\hat{a} + \triangle_b\hat{b}^\dagger\hat{b} + \triangle_c\hat{c}^\dagger\hat{c} + g(\hat{a}^{\dagger 2}\hat{b}\hat{c} + \hat{a}^2\hat{b}^\dagger\hat{c}^\dagger) \\ & + \triangle_e\hat{\sigma}_+\hat{\sigma}_- + J(\hat{a}^\dagger\hat{\sigma}_- + \hat{\sigma}_+\hat{a}) + F_a(\hat{a}^\dagger + \hat{a}),\end{aligned} \tag{2}$$

where $\triangle_{a/b/c} = \omega_{a/b/c} - \omega_l$ is the detuning between the cavity mode $a/b/c$ and driving light field, and $\triangle_e = \omega_e - \omega_l$ is the detuning between the atom and the driving field. For simplicity, we only consider that $2\omega_a = \omega_b + \omega_c$ and the atom is resonant with the cavity mode $\omega_a = \omega_e$. That is, $2\triangle_a = \triangle_b + \triangle_c$, and $\triangle_a = \triangle_e$.

III. ANALYTICAL CONDITIONS FOR PHOTON BLOCKADE

In the weak-driving limit, the matrix form of the total Hamiltonian of this system could be obtained in different subspaces. In the weak-driving limit, the interaction terms between different subspaces are close to zero, so the eigenfrequencies of the Hamiltonian could be obtained by diagonalizing the Hamiltonian of the system in the corresponding subspaces. We choose the states $|g, 1, 0, 0\rangle$ and $|e, 0, 0, 0\rangle$ to form a closed space, so then the Hamiltonian of the system can be written as

$$\hat{H}^{(1)} = \begin{pmatrix} \triangle_a & J \\ J & \triangle_e \end{pmatrix}. \tag{3}$$

The Fock-state basis of this system has been given in the form $|z, n_a, n_b, n_c\rangle$, where z represents the state of the atom and $|n_a\rangle$, $|n_b\rangle$, $|n_c\rangle$ denote the photon numbers of modes a, b, c, respectively. By diagonalization, we obtain the eigenfrequencies of the first excited state as

$$\omega_\pm^{(1)} = \triangle_a \pm J. \tag{4}$$

Similarly, we could obtain the eigenfrequencies of the second and third excited states by diagonalizing the Hamiltonian of system in the corresponding subspaces. By selecting $|g, 2, 0, 0\rangle$, $|g, 0, 1, 1\rangle$, and $|e, 1, 0, 0\rangle$ as the closed space, we get the Hamiltonian of the system in the subspace as

$$\hat{H}^{(2)} = \begin{pmatrix} 2\triangle_a & \sqrt{2}g & \sqrt{2}J \\ \sqrt{2}g & \triangle_b + \triangle_c & 0 \\ \sqrt{2}J & 0 & \triangle_a + \triangle_e \end{pmatrix}. \tag{5}$$

Then we get the eigenfrequencies of the second excited state after diagonalization as

$$\omega_\pm^{(2)} = 2\triangle_a \pm \sqrt{2g^2 + 2J^2}, \quad \omega_0^{(2)} = 2\triangle_a. \tag{6}$$

By choosing the states $|g, 1, 1, 1\rangle$, $|e, 0, 1, 1\rangle$, $|e, 2, 0, 0\rangle$, and $|g, 3, 0, 0\rangle$ as the closed space, the Hamiltonian of the system in the subspace could be rewritten as

$$\hat{H}^{(3)} = \begin{pmatrix} \triangle_b + \triangle_c + \triangle_e & J & \sqrt{2}g & 0 \\ J & \triangle_b + \triangle_c + \triangle_a & 0 & \sqrt{6}g \\ \sqrt{2}g & 0 & 2\triangle_a + \triangle_e & \sqrt{3}J \\ 0 & \sqrt{6}g & \sqrt{3}J & 3\triangle_a \end{pmatrix}. \tag{7}$$

Then the eigenfrequencies of the third excited state after diagonalization are obtained as

$$\omega_{\pm\pm}^{(3)} = 3\triangle_a \pm \sqrt{\tfrac{1}{2}[A \pm \sqrt{A^2 - 4B}]}, \tag{8}$$

where $A = 4J^2 + 6gJ + 2g^2$ and $B = 3J^4 - 12g^2J^2 + 12g^4$.

So we get the energy-level structure of the composite system. As given in Eqs. (4) and (6), the energy-level splitting of the first excited state only depends on the atom-cavity coupling strength J, while the energy-level splitting of the second excited state depends on both the atom-cavity coupling strength J and the four-wave-mixing interaction g. The energy-level diagrams of this system are shown in Figs. 2 and 3. Figure 2 shows the energy-level diagram of this system when the four-wave-mixing interaction g and the atom-cavity coupling strength J are not equal, i.e., $g \neq J$. Figure 3 gives the energy-level diagram of this system when the four-wave-mixing interaction g and the atom-cavity coupling strength J are consistent with each other, i.e., $g = J$. The physical mechanism of the formation of a conventional photon blockade is the anharmonic energy ladder. For $g \neq J$, as shown in Fig. 2, if the transition of $0 \to \omega_\pm^{(1)}$ is resonant, the transition from

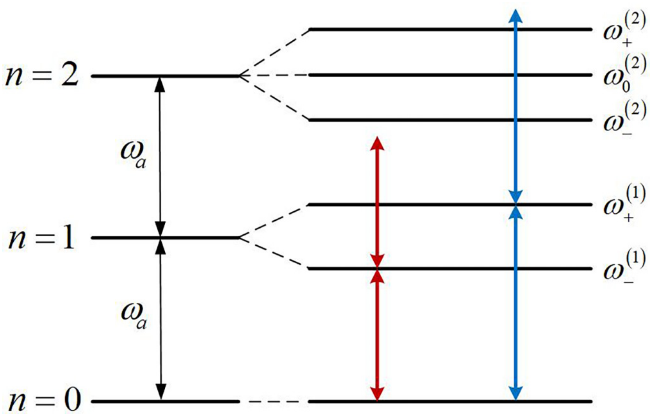

FIG. 2. Schematic energy-level diagram of a four-wave-mixing system embedded with a two-level atom for $g \neq J$. Under this condition, $\omega_{\pm}^{(2)} \neq 2\omega_{\pm}^{(1)}$. If the transition of $0 \to \omega_{\pm}^{(1)}$ is resonant, the transition from $\omega_{\pm}^{(1)}$ to $\omega_{\pm}^{(2)}$ is detuning.

$\omega_{\pm}^{(1)}$ to $\omega_{\pm}^{(2)}$ is detuning. Thus, a one-photon blockade could be realized in this system when the external driving frequency satisfies the resonant condition. Then we could get the optimal analytical condition for the one-photon blockade as

$$\triangle_a = \pm J. \tag{9}$$

For $g = J$, by comparing Eqs. (4) and (6), we can get $\omega_{\pm}^{(2)} = 2\omega_{\pm}^{(1)}$. As shown in Fig. 3, if the transition of $0 \to \omega_{\pm}^{(1)}$ is resonant, the transition from $\omega_{\pm}^{(1)}$ to $\omega_{\pm}^{(2)}$ is resonant and the transition from $\omega_{\pm}^{(2)}$ to $\omega_{\pm\pm}^{(3)}$ is detuning. Thus, a two-photon blockade could be realized in this system when the external driving frequency satisfies the resonant condition. Then we could get the optimal analytical condition for the two-photon blockade as

$$\triangle_a = \pm J. \tag{10}$$

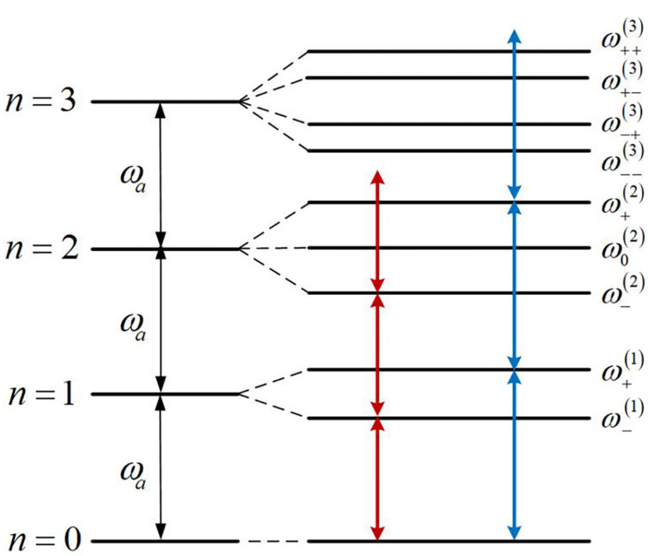

FIG. 3. Schematic energy-level diagram of a four-wave-mixing system embedded with a two-level atom for $g = J$. Under this condition, $\omega_{\pm}^{(2)} = 2\omega_{\pm}^{(1)}$. If the transition of $0 \to \omega_{\pm}^{(1)}$ is resonant, the transition from $\omega_{\pm}^{(1)}$ to $\omega_{\pm}^{(2)}$ is resonant and the transition from $\omega_{\pm}^{(2)}$ to $\omega_{\pm\pm}^{(3)}$ is detuning.

IV. NUMERICAL ANALYSIS FOR PHOTON BLOCKADE

A. Numerical analysis method

Usually, we could know whether or not the photon blockade happens by using a zero-delay-time correlation function which describes the statistical properties of photons. The one-photon blockade will occur when the two-order correlation function $g^{(2)}(0) < 1$, while the two-photon blockade happens when the three-order correlation function $g^{(3)}(0) < 1$ and the two-order correlation function $g^{(2)}(0) > 1$. The two-order and three-order correlation functions are defined as

$$g^{(2)}(0) = \frac{\mathrm{Tr}(\hat{a}^\dagger \hat{a}^\dagger \hat{a}\hat{a}\hat{\rho}_{\mathrm{ss}})}{[\mathrm{Tr}(\hat{a}^\dagger \hat{a}\hat{\rho}_{\mathrm{ss}})]^2}, \tag{11}$$

$$g^{(3)}(0) = \frac{\mathrm{Tr}(\hat{a}^\dagger \hat{a}^\dagger \hat{a}^\dagger \hat{a}\hat{a}\hat{a}\hat{\rho}_{\mathrm{ss}})}{[\mathrm{Tr}(\hat{a}^\dagger \hat{a}\hat{\rho}_{\mathrm{ss}})]^3}, \tag{12}$$

where $\hat{\rho}_{\mathrm{ss}}$ is the steady-state density matrix, which could be solved from the master equation, that is,

$$\begin{aligned}\frac{\partial \hat{\rho}}{\partial t} = & -i[\hat{H}_{\mathrm{eff}}, \hat{\rho}] + \frac{\gamma}{2}(\bar{n}_{\mathrm{th}}+1)(2\hat{\sigma}\hat{\rho}\hat{\sigma}^\dagger - \hat{\sigma}^\dagger\hat{\sigma}\hat{\rho} - \hat{\rho}\hat{\sigma}^\dagger\hat{\sigma}) \\ & + \frac{\kappa_a}{2}(\bar{n}_{\mathrm{th}}+1)(2\hat{a}\hat{\rho}\hat{a}^\dagger - \hat{a}^\dagger\hat{a}\hat{\rho} - \hat{\rho}\hat{a}^\dagger\hat{a}) \\ & + \frac{\kappa_b}{2}(\bar{n}_{\mathrm{th}}+1)(2\hat{b}\hat{\rho}\hat{b}^\dagger - \hat{b}^\dagger\hat{b}\hat{\rho} - \hat{\rho}\hat{b}^\dagger\hat{b}) \\ & + \frac{\kappa_c}{2}(\bar{n}_{\mathrm{th}}+1)(2\hat{c}\hat{\rho}\hat{c}^\dagger - \hat{c}^\dagger\hat{c}\hat{\rho} - \hat{\rho}\hat{c}^\dagger\hat{c}) \\ & + \frac{\gamma}{2}\bar{n}_{\mathrm{th}}(2\hat{\sigma}\hat{\rho}\hat{\sigma}^\dagger - \hat{\sigma}^\dagger\hat{\sigma}\hat{\rho} - \hat{\rho}\hat{\sigma}^\dagger\hat{\sigma}) \\ & + \frac{\kappa_a}{2}\bar{n}_{\mathrm{th}}(2\hat{a}\hat{\rho}\hat{a}^\dagger - \hat{a}^\dagger\hat{a}\hat{\rho} - \hat{\rho}\hat{a}^\dagger\hat{a}) \\ & + \frac{\kappa_b}{2}\bar{n}_{\mathrm{th}}(2\hat{b}\hat{\rho}\hat{b}^\dagger - \hat{b}^\dagger\hat{b}\hat{\rho} - \hat{\rho}\hat{b}^\dagger\hat{b}) \\ & + \frac{\kappa_c}{2}\bar{n}_{\mathrm{th}}(2\hat{c}\hat{\rho}\hat{c}^\dagger - \hat{c}^\dagger\hat{c}\hat{\rho} - \hat{\rho}\hat{c}^\dagger\hat{c}),\end{aligned} \tag{13}$$

where κ_a, κ_b, and κ_c denote the decay rates of modes a, b, and c, respectively, and γ is the atomic spontaneous emission rate. The $\bar{n}_{\mathrm{th}}$ denotes the number of thermal photons, and it obeys $\bar{n}_{\mathrm{th}} = \{\hbar\omega/(\kappa_B T) - 1\}^{-1}$, where κ_B denotes the Boltzmann constant and T is the reservoir temperature at thermal equilibrium. For convenience, in the following numerical simulations, the decay rates of the modes are assumed to be equal, i.e., $\kappa_a = \kappa_b = \kappa_c = \kappa$, and all the parameters are rescaled with respect to the decay rate κ.

B. Numerical analysis of a one-photon blockade in cavity *a*

The logarithmic plot of a two-order correlation function $g^{(2)}(0)$ as a function of $\triangle_a/\kappa$ is shown in Fig. 4. Here, we set $F_a/\kappa = 0.01$, $J/\kappa = 5$, $g/\kappa = 10$, $\gamma = (1/16)\kappa$. The numerical result shows that a one-photon blockade can be realized in cavity a. As is shown in Fig. 4, the values of $g^{(2)}(0)$ could be lower than one, which means that a strong one-photon blockade could be realized in cavity a. In addition, the optimal

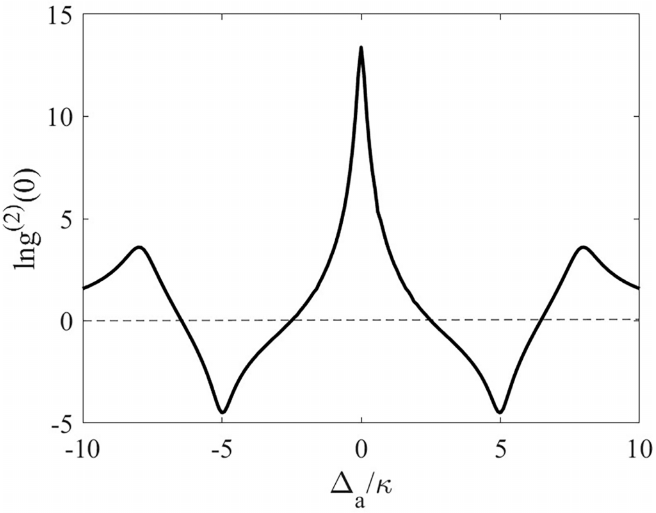

FIG. 4. Logarithmic plot of a two-order correlation function as a function of $\triangle_a/\kappa$ with $F_a/\kappa = 0.01$, $J/\kappa = 5$, $g/\kappa = 10$, $\gamma = (1/16)\kappa$.

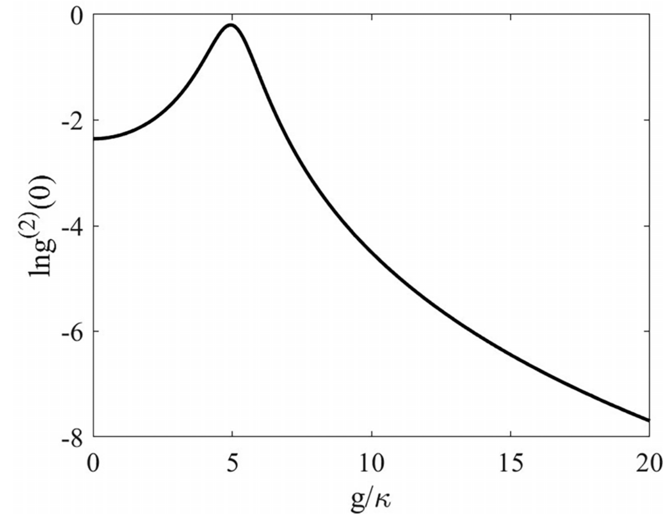

FIG. 6. Logarithmic plot of a two-order correlation function as a function of the four-wave-mixing interaction g with $\triangle_a/\kappa = J/\kappa = 5$, $F_a/\kappa = 0.01$, $\gamma = (1/16)\kappa$.

blockade position is at $\triangle_a/\kappa = \pm 5$, which is consistent with the optimal analytic condition given in Eq. (9). They result from the anharmonic energy ladder of the system, as shown in Fig. 2. With the same parameters, we plot the average photon number N_a as a function of $\triangle_a/\kappa$, as shown in Fig. 5. The result further indicates the realization of a one-photon blockade in cavity a.

We further plot the second-order correlation function $g^{(2)}(0)$ versus the system parameters to study their influences on the one-photon blockade effect. Figure 6 shows the logarithmic plot of $g^{(2)}(0)$ as a function of the four-wave-mixing interaction g with $\triangle_a/\kappa = J/\kappa = 5$, $F_a/\kappa = 0.01$, $\gamma = (1/16)\kappa$. As is seen from Fig. 6, evidently the one-photon blockade effect in cavity a depends on g. When g is smaller than 5, that is, $g < J$, $g^{(2)}(0)$ increases with g. When g is greater than 5, that is, $g > J$, $g^{(2)}(0)$ oppositely decreases with g. That is, when the value of g is closer to the value of J, the value of $g^{(2)}(0)$ becomes larger and the blockade effect becomes worse. The logarithmic plot of $g^{(2)}(0)$ as a function of the atom-cavity coupling strength J is shown in Fig. 7 with $\triangle_a/\kappa = J/\kappa$, $g/\kappa = 5$, $F_a/\kappa = 0.01$, $\gamma = (1/16)\kappa$. As shown in Fig. 6, similarly, when the value of J is closer to the value of g, the value of $g^{(2)}(0)$ becomes larger and the blockade effect becomes worse. The results above show that a one-photon blockade effect in cavity a could be facilitated largely by adjusting the four-wave-mixing interaction g and the atom-cavity coupling strength J.

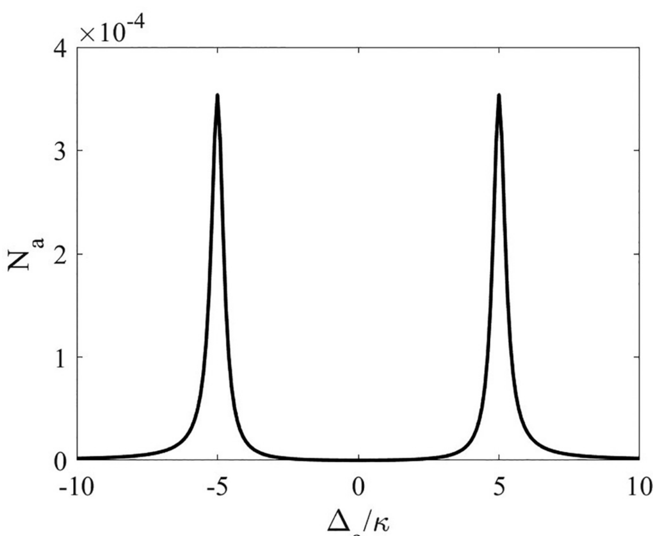

FIG. 5. Plot of the average photon number N_a as a function of $\triangle_a/\kappa$ with $F_a/\kappa = 0.01$, $J/\kappa = 5$, $g/\kappa = 10$, $\gamma = (1/16)\kappa$.

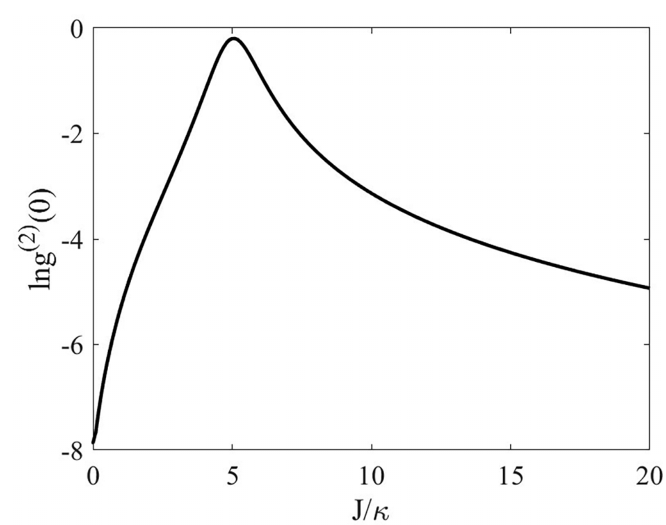

FIG. 7. Logarithmic plot of a two-order correlation function as a function of the atom-cavity coupling strength J, with $\triangle_a/\kappa = J/\kappa$, $g/\kappa = 5$, $F_a/\kappa = 0.01$, $\gamma = (1/16)\kappa$.

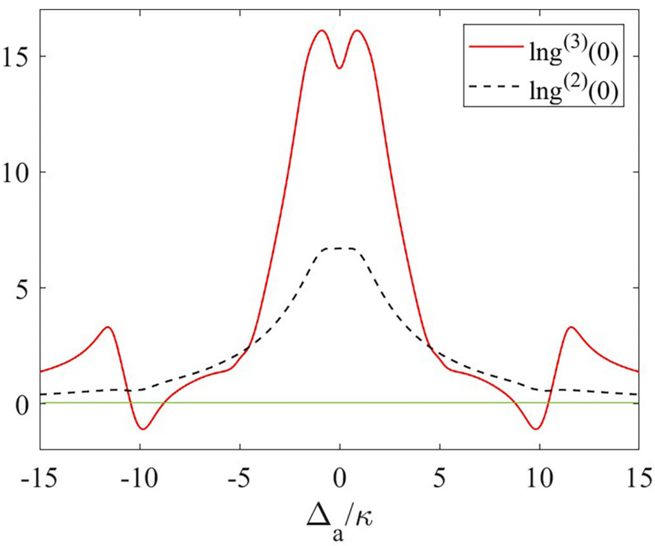

FIG. 8. Logarithmic plots of a two-order correlation function (black dashed line) and a third-order correlation function (red solid line) as a function of $\triangle_a/\kappa$ with $J/\kappa = 10$, $g/\kappa = 10$, $F_a/\kappa = 0.32$, and $\gamma/\kappa = 1$.

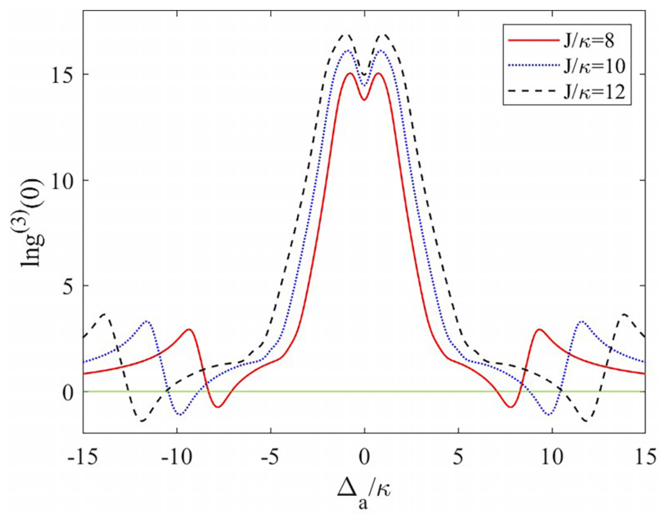

FIG. 10. Logarithmic plot of a third-order correlation function as a function of $\triangle_a/\kappa$ with $J/\kappa = g/\kappa$, $F_a/\kappa = 0.32$, and $\gamma/\kappa = 1$. The values of J for the red solid line, blue dotted line, and black dashed line are $J/\kappa = 8$, $J/\kappa = 10$, and $J/\kappa = 12$, respectively.

C. Numerical analysis of a two-photon blockade in cavity *a*

The logarithmic plots of a two-order correlation function $g^{(2)}(0)$ (black dashed line) and a third-order correlation function $g^{(3)}(0)$ (red solid line) varying with $\triangle_a/\kappa$ are shown in Fig. 8. Here, $J/\kappa = 10$, $g/\kappa = 10$, $F_a/\kappa = 0.32$, and $\gamma/\kappa = 1$. As is shown in Fig. 8, the values of $g^{(2)}(0)$ could be higher than one and the values of $g^{(3)}(0)$ are lower than one simultaneously, which means that a strong two-photon blockade could be realized in cavity a. In addition, the optimal blockade position is at $\triangle_a/\kappa = \pm 10$, which is consistent with the optimal analytic condition given in Eq. (10). They result from the anharmonic energy ladder of the system, as shown in Fig. 3. With the same parameters, we plot the average photon number N_a as a function of $\triangle_a/\kappa$, as shown in Fig. 9. The result further indicates the realization of a two-photon blockade in cavity a.

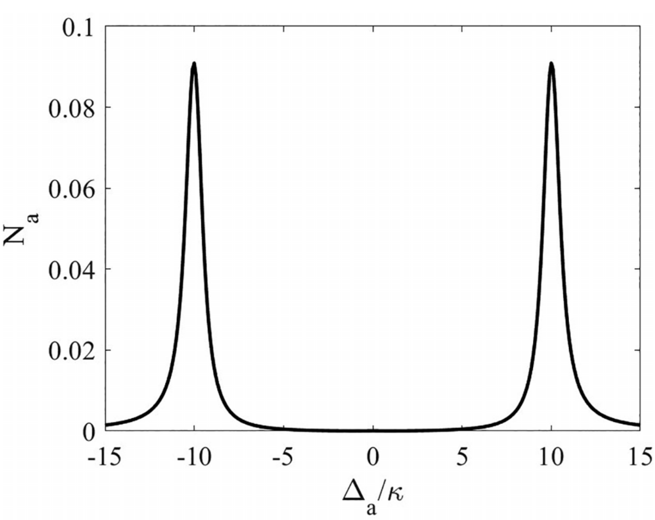

FIG. 9. Plot of average photon number N_a as a function of $\triangle_a/\kappa$ with $J/\kappa = 10$, $g/\kappa = 10$, $F_a/\kappa = 0.32$, and $\gamma/\kappa = 1$.

Figure 10 shows the effect of the four-wave-mixing interaction g and the atom-cavity coupling strength J on the two-photon blockade. In Fig. 10, we logarithmically plot the third-order correlation function $g^{(3)}(0)$ as a function of $\triangle_a/\kappa$ under different values of J/κ, and $g/\kappa = J/\kappa$. The values of J/κ are $J/\kappa = 8$ (red solid line), $J/\kappa = 10$ (blue dotted line), and $J/\kappa = 12$ (black dashed line), respectively. The shared parameter is $F_a/\kappa = 0.32$ and $\gamma/\kappa = 1$. As is seen from Fig. 10, a two-photon blockade could be realized for different values of J/κ, and it gets stronger with increasing J/κ.

All the results show that both one-photon and two-photon blockades could be realized in this composite system. In addition, for the practical realization of a photon blockade of this model, we could adopt different potential systems based on JC coupling [41] and four-wave mixing, for example, coupled photonic wire nanocavities [59], subwavelength grated resonators [60], and double-quantum-well microcavities [61], and the parameters we adopt are feasible experimentally [34,62]. For example, the atom-cavity coupling strength J could be around $J/\kappa = 10$ experimentally [34]. Furthermore, the order of magnitude for four-wave-mixing interaction we adopt is $g/\kappa = 10$, and it is a realistic estimate. The value of it could be reduced at the cost of increasing $g^{(2)}(0)$ or $g^{(3)}(0)$. Thus, the proposed system could be used to obtain single-photon or two-photon sources or devices.

Finally, in order to find the advantages of this system to realize a photon blockade, we compare our results with that in similar systems given in Refs. [41,58]. The proposed model in this paper could be considered as a composite model of the JC model and the four-wave-mixing model. For $g = 0$, the hybrid system is reduced to a JC model, and Ref. [41] shows the photon blockade in the JC model. For $J = 0$, the hybrid system is reduced to a four-wave-mixing model, and Ref. [58] gives the photon blockade in the four-wave-mixing model. Figures 11(a)–11(c) show the energy ladder in the hybrid

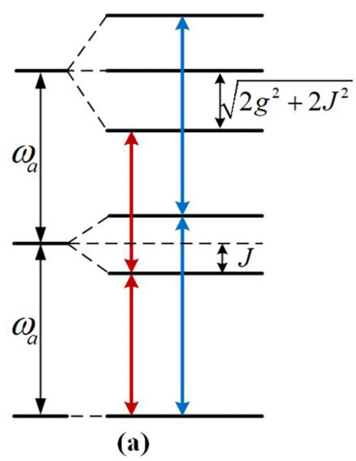

FIG. 11. (a) Schematic energy-level diagram of the hybrid system (for $J = g$). (b) Schematic energy-level diagram of the JC model. (c) Schematic energy-level diagram of the four-wave-mixing model.

system (for $g = J$), the JC model, and the four-wave-mixing model, respectively. It should be noted that here we focus on the CPB effects in the three different systems under the same driving condition, that is, driving the cavity mode a only. As shown in Fig. 11(a), in the hybrid system, the energy-level splitting of the first excited state only depends on the atom-cavity coupling strength J, while the energy-level shift of the second excited state depends on both the atom-cavity coupling strength J and the four-wave-mixing interaction g. Thus, the system could realize a two-photon blockade when $g = J$. As shown in Fig. 11(b), in the JC model, both the energy-level splittings of the first excited state and the second excited state only depend on J, so only a one-photon blockade could exist under this driving condition [41]. As shown in Fig. 11(c), in the four-wave-mixing model, the energy-level splitting of the second excited state only depends on g, so only a one-photon blockade could be realized under this driving condition [58].

A comparison of the photon blockade effect in the present scheme with that in Refs. [41,58] under this driving condition is also shown in Table I. As is seen in Table I, different from the results in Refs. [41,58], the scheme we adopt in this paper could both realize a one-photon blockade and two-photon blockade, which may lead to wide applications in quantum-nonlinear optics such as a single-photon or multiphoton source. Moreover, for a one-photon blockade, compared with the scheme adopted in Ref. [41], the system we choose here could have a more obvious one-photon blockade effect under similar parameters. Compared with the scheme adopted in Ref. [58], the system we choose here could block two different frequencies of photons in one system.

V. CONCLUSION

In this paper, we have investigated the photon blockade effect of a four-wave-mixing system embedded with a two-level atom. Through an analytical analysis, we find that both one-photon and two-photon blockades could be realized in this system with different values of the atomic coupling strength and the four-wave-mixing interaction. When the two values are not equal, a one-photon blockade can be formed, and when the two values are equal, a two-photon blockade can be achieved. Then we investigate the blockade effect numerically by using a master equation and correlation function. Results show that the numerical results are consistent with the analytical conditions. Single-photon and multiphoton blockades could be implemented in this system, which may lead to wide applications in quantum-nonlinear optics such as different photon sources. The results also show that the blockade effect could be facilitated largely by adjusting the parameters of the system. All the results may provide useful references for single-photon and multiphoton sources or the design of devices in future studies.

ACKNOWLEDGMENT

This work is supported by the Natural Science Foundation of Jilin Province under Grant No. YDZJ202101ZYTS030.

TABLE I. Comparison of the photon blockade effect in different schemes.

	J	g	CPB	Optimal blockade condition
Scheme in Ref. [41]	√	None	One-photon blockade	$\triangle_a = \pm J$
Scheme in Ref. [58]	None	√	One-photon blockade	$\triangle_a = 0$
Our scheme	√	√	One-photon blockade ($g \neq J$)	$\triangle_a = \pm J$
			Two-photon blockade ($g = J$)	$\triangle_a = \pm J$

[1] E. Knill, R. Laflamme, and G. J. Milburn, A scheme for efficient quantum computation with linear optics, Nature (London) **409**, 46 (2001).

[2] B. Lounis and M. Orrit, Single-photon sources, Rep. Prog. Phys. **68**, 1129 (2005).

[3] H. Wang, Y. He, Y.-H. Li, Z.-E. Su, B. Li, H.-L. Huang, X. Ding, M.-C. Chen, C. Liu, J. Qin *et al.*, High-efficiency multiphoton boson sampling, Nat. Photon. **11**, 361 (2017).

[4] D. E. Chang, V. Vuletić, and M. D. Lukin, Quantum nonlinear optics—photon by photon, Nat. Photon. **8**, 685 (2014).

[5] P. Kok, W. J. Munro, K. Nemoto, T. C. Ralph, J. P. Dowling, and G. J. Milburn, Linear optical quantum computing with photonic qubits, Rev. Mod. Phys. **79**, 135 (2007); Publisher's Note: Linear optical quantum computing with photonic qubits [Rev. Mod. Phys. 79, 135 (2007)], **79**, 797(E) (2007).

[6] V. Scarani, H. Bechmann-Pasquinucci, N. J. Cerf, M. Dušek, N. Lütkenhaus, and M. Peev, The security of practical quantum key distribution, Rev. Mod. Phys. **81**, 1301 (2009).

[7] R. H. Hadfield, Single-photon detectors for optical quantum information applications, Nat. Photon. **3**, 696 (2009).

[8] X. Gu, L. Chen, and M. Krenn, Quantum experiments and hypergraphs: Multiphoton sources for quantum interference, quantum computation, and quantum entanglement, Phys. Rev. A **101**, 033816 (2020).

[9] A. Imamoḡlu, H. Schmidt, G. Woods, and M. Deutsch, Strongly interacting photons in a nonlinear cavity, Phys. Rev. Lett. **79**, 1467 (1997).

[10] H. Wang, X. Gu, Y. X. Liu, A. Miranowicz, and F. Nori, Tunable photon blockade in a hybrid system consisting of an optomechanical device coupled to a two-level system, Phys. Rev. A **92**, 033806 (2015).

[11] H. Flayac and V. Savona, Unconventional photon blockade, Phys. Rev. A **96**, 053810 (2017).

[12] T. C. H. Liew and V. Savona, Single photons from coupled quantum modes, Phys. Rev. Lett. **104**, 183601 (2010).

[13] P. Yang, M. Li, X. Han, H. He, G. Li, C.-L. Zou, P. Zhang, Y. Qian, and T. Zhang, Non-reciprocal cavity polariton with atoms strongly coupled to optical cavity, Laser Photon. Rev. **17**, 2200574 (2023).

[14] A. Miranowicz, M. Paprzycka, Y. X. Liu, J. Bajer, and F. Nori, Two-photon and three-photon blockades in driven nonlinear systems, Phys. Rev. A **87**, 023809 (2013).

[15] A. Graf, S. D. Rogers, J. Staffa, U. A. Javid, D. H. Griffith, and Q. Lin, Nonreciprocity in photon pair correlations of classically reciprocal systems, Phys. Rev. Lett. **128**, 213605 (2022).

[16] R. Huang, Ş. Özdemir, J.-Q. Liao, F. Minganti, L.-M. Kuang, F. Nori, and H. Jing, Exceptional photon blockade: Engineering photon blockade with chiral exceptional points, Laser Photon. Rev. **16**, 2100430 (2022).

[17] Y. Zuo, R. Huang, L.-M. Kuang, X.-W. Xu, and H. Jing, Loss-induced suppression, revival, and switch of photon blockade, Phys. Rev. A **106**, 043715 (2022).

[18] B. Li, R. Huang, X. Xu, A. Miranowicz, and H. Jing, Nonreciprocal unconventional photon blockade in a spinning optomechanical system, Photon. Res. **7**, 630 (2019).

[19] C. Lang, D. Bozyigit, C. Eichler, L. Steffen, J. M. Fink, A. A. Abdumalikov Jr., M. Baur, S. Filipp, M. P. da Silva, A. Blais, and A. Wallraff, Observation of resonant photon blockade at microwave frequencies using correlation function measurements, Phys. Rev. Lett. **106**, 243601 (2011).

[20] Y.-X. Liu, X.-W. Xu, A. Miranowicz, and F. Nori, From blockade to transparency: Controllable photon transmission through a circuit-QED system, Phys. Rev. A **89**, 043818 (2014).

[21] M. Leib and M. J. Hartmann, Bose–Hubbard dynamics of polaritons in a chain of circuit quantum electrodynamics cavities, New J. Phys. **12**, 093031 (2010).

[22] P. Rabl, Photon blockade effect in optomechanical systems, Phys. Rev. Lett. **107**, 063601 (2011).

[23] X.-W. Xu and Y.-J. Li, Antibunching photons in a cavity coupled to an optomechanical system, J. Phys. B: At. Mol. Opt. Phys. **46**, 035502 (2013).

[24] J.-Q. Liao and F. Nori, Photon blockade in quadratically coupled optomechanical systems, Phys. Rev. A **88**, 023853 (2013).

[25] H. Jabri and H. Eleuch, Enhanced unconventional photon-blockade effect in one-and two-qubit cavities interacting with nonclassical light, Phys. Rev. A **106**, 023704 (2022).

[26] Y. Zhang, J. Zhang, and C.-s. Yu, Photon statistics on the extreme entanglement, Sci. Rep. **6**, 24098 (2016).

[27] K. Almutairi, R. Tanaś, and Z. Ficek, Generating two-photon entangled states in a driven two-atom system, Phys. Rev. A **84**, 013831 (2011).

[28] C. Sukumar and B. Buck, Multi-phonon generalisation of the Jaynes-Cummings model, Phys. Lett. A **83**, 211 (1981).

[29] S. Singh, Field statistics in some generalized Jaynes-Cummings models, Phys. Rev. A **25**, 3206 (1982).

[30] K. Ng, C. Lo, and K. Liu, Exact eigenstates of the two-photon Jaynes-Cummings model with the counter-rotating term, Eur. Phys. J. D **6**, 119 (1999).

[31] J.-Q. Liao and C. K. Law, Correlated two-photon transport in a one-dimensional waveguide side-coupled to a nonlinear cavity, Phys. Rev. A **82**, 053836 (2010).

[32] G. H. Hovsepyan, A. R. Shahinyan, and G. Y. Kryuchkyan, Multiphoton blockades in pulsed regimes beyond stationary limits, Phys. Rev. A **90**, 013839 (2014).

[33] S. Ferretti, L. C. Andreani, H. E. Türeci, and D. Gerace, Photon correlations in a two-site nonlinear cavity system under coherent drive and dissipation, Phys. Rev. A **82**, 013841 (2010).

[34] C. Hamsen, K. N. Tolazzi, T. Wilk, and G. Rempe, Two-photon blockade in an atom-driven cavity QED system, Phys. Rev. Lett. **118**, 133604 (2017).

[35] R. Huang, A. Miranowicz, J.-Q. Liao, F. Nori, and H. Jing, Nonreciprocal photon blockade, Phys. Rev. Lett. **121**, 153601 (2018).

[36] J. Tang, Y. Deng, and C. Lee, Tunable photon blockade with a single atom in a cavity under electromagnetically induced transparency, Photon. Res. **9**, 1226 (2021).

[37] I. I. Smolyaninov, A. V. Zayats, A. Gungor, and C. C. Davis, Single-photon tunneling via localized surface plasmons, Phys. Rev. Lett. **88**, 187402 (2002).

[38] W. Leoński and R. Tanaś, Possibility of producing the one-photon state in a kicked cavity with a nonlinear Kerr medium, Phys. Rev. A **49**, R20 (1994).

[39] H. Zheng, D. J. Gauthier, and H. U. Baranger, Cavity-free photon blockade induced by many-body bound states, Phys. Rev. Lett. **107**, 223601 (2011).

[40] T. E. Lee and M. C. Cross, Quantum-classical transition of correlations of two coupled cavities, Phys. Rev. A **88**, 013834 (2013).

[41] K. M. Birnbaum, A. Boca, R. Miller, A. D. Boozer, T. E. Northup, and H. J. Kimble, Photon blockade in an

optical cavity with one trapped atom, Nature (London) **436**, 87 (2005).
[42] H. Lin, X. Wang, Z. Yao, and D. Zou, Kerr-nonlinearity enhanced conventional photon blockade in a second-order nonlinear system, Opt. Express **28**, 17643 (2020).
[43] C. Vaneph, A. Morvan, G. Aiello, M. Féchant, M. Aprili, J. Gabelli, and J. Estève, Observation of the unconventional photon blockade in the microwave domain, Phys. Rev. Lett. **121**, 043602 (2018).
[44] H. J. Snijders, J. A. Frey, J. Norman, H. Flayac, V. Savona, A. C. Gossard, J. E. Bowers, M. P. van Exter, D. Bouwmeester, and W. Löffler, Observation of the unconventional photon blockade, Phys. Rev. Lett. **121**, 043601 (2018).
[45] S. Dufferwiel, F. Fras, A. Trichet, P. Walker, F. Li, L. Giriunas, M. Makhonin, L. Wilson, J. Smith, E. Clarke *et al.*, Strong exciton-photon coupling in open semiconductor microcavities, Appl. Phys. Lett. **104**, 192107 (2014).
[46] H. Z. Shen, Y. H. Zhou, and X. X. Yi, Tunable photon blockade in coupled semiconductor cavities, Phys. Rev. A **91**, 063808 (2015).
[47] D. Gerace and V. Savona, Unconventional photon blockade in doubly resonant microcavities with second-order nonlinearity, Phys. Rev. A **89**, 031803(R) (2014).
[48] S. Ferretti and D. Gerace, Single-photon nonlinear optics with Kerr-type nanostructured materials, Phys. Rev. B **85**, 033303 (2012).
[49] D. G. Angelakis, M. F. Santos, and S. Bose, Photon-blockade-induced Mott transitions and XY spin models in coupled cavity arrays, Phys. Rev. A **76**, 031805(R) (2007).
[50] A. Faraon, I. Fushman, D. Englund, N. Stoltz, P. Petroff, and J. Vučković, Coherent generation of non-classical light on a chip via photon-induced tunnelling and blockade, Nat. Phys. **4**, 859 (2008).
[51] J. Tang, W. Geng, and X. Xu, Quantum interference induced photon blockade in a coupled single quantum dot-cavity system, Sci. Rep. **5**, 9252 (2015).
[52] X. Liang, Z. Duan, Q. Guo, S. Guan, M. Xie, and C. Liu, Photon blockade in a bimode nonlinear nanocavity embedded with a quantum dot, Phys. Rev. A **102**, 053713 (2020).
[53] M.-T. Cheng, X.-S. Ma, M.-T. Ding, Y.-Q. Luo, and G.-X. Zhao, Single-photon transport in one-dimensional coupled-resonator waveguide with local and nonlocal coupling to a nanocavity containing a two-level system, Phys. Rev. A **85**, 053840 (2012).
[54] H. Lin, Compound photon blockade based on three mode system, arXiv:2201.01127.
[55] F. Zou, X.-Y. Zhang, X.-W. Xu, J.-F. Huang, and J.-Q. Liao, Multiphoton blockade in the two-photon Jaynes-Cummings model, Phys. Rev. A **102**, 053710 (2020).
[56] A. Majumdar and D. Gerace, Single-photon blockade in doubly resonant nanocavities with second-order nonlinearity, Phys. Rev. B **87**, 235319 (2013).
[57] Y. H. Zhou, X. Y. Zhang, Q. C. Wu, B. L. Ye, Z.-Q. Zhang, D. D. Zou, H. Z. Shen, and C.-P. Yang, Conventional photon blockade with a three-wave mixing, Phys. Rev. A **102**, 033713 (2020).
[58] Z.-X. Wang, H. Yang, X.-Q. Wang, H.-Y. Lin, and Z.-H. Yao, Conventional photon blockade in a four-wave mixing system with Kerr nonlinearity, Phys. Scr. **98**, 035108 (2023).
[59] S. Azzini, D. Grassani, M. Galli, D. Gerace, M. Patrini, M. Liscidini, P. Velha, and D. Bajoni, Stimulated and spontaneous four-wave mixing in silicon-on-insulator coupled photonic wire nano-cavities, Appl. Phys. Lett. **103**, 031117 (2013).
[60] O. Kyriienko, E. A. Ostrovskaya, O. A. Egorov, I. A. Shelykh, and T. C. H. Liew, Bistability in microcavities with incoherent optical or electrical excitation, Phys. Rev. B **90**, 125407 (2014).
[61] G. Christmann, A. Askitopoulos, G. Deligeorgis, Z. Hatzopoulos, S. I. Tsintzos, P. G. Savvidis, and J. J. Baumberg, Oriented polaritons in strongly-coupled asymmetric double quantum well microcavities, Appl. Phys. Lett. **98**, 081111 (2011).
[62] Y. Sherkunov, D. M. Whittaker, and V. I. Falko, Optical source of individual pairs of colour-conjugated photons, Sci. Rep. **7**, 11418 (2017).